Full text at publisher | Export | Add To Marked List

Comprehensive growth and characterization study of GeOx/Si

By Baghdedi, D (Baghdedi, Dhouha) [1] , [2] , [3] ; Hopoglu, H (Hopoglu, Hicret) [2] , [3] ; Saritas, S (Saritas, Sevda) [4] ; Demir, I (Demir, Ilkay) [3] , [5] ; Altuntas, I (Altuntas, Ismail) [3] , [5] ; Abdelmoula, N (Abdelmoula, Najmeddine) [1] ; Gür, E (Gur, Emre) [6] ; Tüzemen, ES (Tuzemen, Ebru Senadim) [2] , [3]

View Web of Science ResearcherID and ORCID (provided by Clarivate)

Source JOURNAL OF MOLECULAR STRUCTURE

Volume: 1274 Part: 1

DOI: 10.1016/j.molstruc.2022.134398

Article Number 134398

Published FEB 15 2023

Early Access OCT 2022

Indexed 2023-01-23

Document Type Article

Abstract In this study, the reactive radio frequency magnetron sputtering (RFMS) method under varying thickness was used to deposit GeOx on Si substrate at room temperature. The effect of thickness on the structural and optical properties of high-quality germanium dioxide (GeO2) thin films have been investigated by experimental. Structural properties were investigated using X-ray diffraction. It has been observed that the peak intensity of (113) reflection is the highest in the spectrum of 240.22 nm thickness and using scanning electron microscope (SEM) to calculate thickness of different samples. Reflection measurement, which is one of its optical properties, was measured with an optical spectrophotometer. It has been ob-served that as the thickness increases, the total reflectance changes. The absorption coefficient was calcu-lated using the diffuse reflection curve. From this point of view, the energy band gap was calculated and it was seen that it varies between 4.1 eV and 4.4 eV. As a result, it was observed that the energy band gap increased as the thickness increased. And using spectroscopic ellipsometry to calculate the thickness of different, refractive index, extinction coefficient, and oscillator parameters. The oscillator energy decrease as the thickness of films increases

Citation Network

In Web of Science Core Colle

1 Citation

Create citation alert

1 Times Cited in All Data

+ See more times cited

25 Cited References

View Related Records →

Citing items by classifica

Breakdown of how this arti mentioned, based on avail context data and snippets item(s).

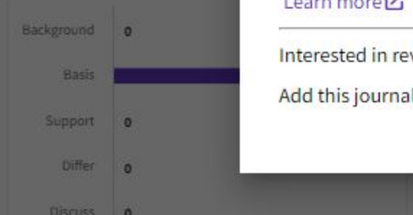

Journal information

JOURNAL OF MOLECULAR STRUCTURE

Publisher name: ELSEVIER

Journal Impact Factor ™

3.8	3.2
2022	Five Year

JCR Category	Category Rank	Category Quartile
CHEMISTRY, PHYSICAL *in SCIE edition*	74/161	Q2

Source: Journal Citation Reports 2022. Learn more

Journal Citation Indicator ™

0.57	0.52
2022	2021

JCI Category	Category Rank	Category Quartile
CHEMISTRY, PHYSICAL *in SCIE edition*	89/172	Q3

The Journal Citation Indicator is a measure of the average Category Normalized Citation Impact (CNCI) of citable items (articles and reviews) published by a journal over a recent three year period. It is used to help you evaluate journals based on other metrics besides the Journal Impact Factor (JIF).

Learn more

Interested in reviewing for this journal?

Add this journal to your reviewer interest list. Add Journal

Journal of Molecular Structure 1272 (2023) 134203

Contents lists available at ScienceDirect

Journal of Molecular Structure

journal homepage: www.elsevier.com/locate/molstr

Effect of Si-doped and undoped inter-layer transition time on the strain-compensated InGaAs/InAlAs QCL active region grown with MOVPE

Izel Perkitel[a,b], Ilkay Demir[1,b,*]

[a] Nanophotonics Research and Application Center, Sivas Cumhuriyet University, 58140 Sivas, Turkey
[b] Department of Nanotechnology Engineering, Sivas Cumhuriyet University, 58140 Sivas, Turkey

ARTICLE INFO

Article history:
Received 16 July 2022
Revised 9 September 2022
Accepted 22 September 2022
Available online 23 September 2022

Keywords:
QCL
MOVPE
XRD
in-situ reflectance
thickness sensitivity

ABSTRACT

In this study, we report the effect of the combination of Si-doped and undoped inter-layer transition time in the strain compensated $In_{0.67}Ga_{0.33}As/In_{0.36}Al_{0.64}As$ quantum cascade laser (QCL) structure grown on InP substrate by Metal Organic Vapor Phase Epitaxy (MOVPE). In situ reflectance spectroscopy and high resolution X-ray diffraction (HRXRD) technique have been used for the analysis of growth steps and crystalline quality of QCL structures, respectively. In addition, since thickness accuracy is very important for QCLs, two different thickness calculation methods have been used in the Global Fit simulation program for detailed thickness accuracy of structures. As a result, optimum values for thickness accuracy have been obtained as 5 and 10 s between undoped and Si-doped layers, respectively, as verified by the two methods.

1. Introduction

Quantum cascade lasers (QCLs) are high-performance light sources operating in the mid-infrared spectral region (3-20 μm) [1,2]. It offers an infrared laser application a unique combination of compact size, high power and efficiency, and design flexibility [3]. QCLs are laser devices bottomed on inter-subband transitions in semiconductor heterostructures [4]. QCLs are ideal nominees for the mid to far-infrared spectral region, as the emission wavelength is identified by the layer width and array and not by the bandgap. QCLs have been of major interest for a range of industrial applications, including infrared imaging and spectroscopy, as well as various defense applications such as range detection and free-space optical communications [5–10].

The superlattices based on the InGaAs/InAlAs heterostructure are mostly used in the construction of QCLs [11–14]. The emission wavelength of lattice-matched InGaAs/InAlAs QCLs with InP substrate covers the infrared region from 3.5 to 24 μm and this gives them the occasion to use them for chemical and biological sensing or spectroscopy application. A particularly up-and-coming area of application for QCLs is gas detection in the 2.9-5.3 μm (first atmospheric window). Besides line-of-sight telecommunications, military countermeasures based on emissions in the first atmospheric window are also of interest [15]. Laser realization inside of this region is particularly difficult due to the large conduction band discontinuity (ΔE_c) required. The most mature material system used for short wavelength QCLs is the strain-compensated InP-based InGaAs/InAlAs [16].

The QCL core includes hundreds of thin layer repetitions with a thickness in the 0.5–10 nm range. The growth of QCLs is crucial in terms of the alloy composition, layer thickness, and heterointerface quality of hundreds of ultrathin epitaxial layers [17]. Molecular beam epitaxy (MBE) is the most used technique when it comes to complex structures. MBE technique supplies a specific composition and very high quality interfaces in individual layers. However, due to the high vacuum need, the MBE technique has lower QCL production capacity and higher cost. Metal Organic Vapor Phase Epitaxy (MOVPE) is another technique used to grow high quality QCL wafers. However, epitaxial growth of such layers with MOVPE technique is very difficult. It is significant to obtain the optimal growth parameters [18]. Growth kinetics depend on various factors such as temperature, process pressure, and flow rate of precursors and they extremely influence the growth of individual layers. There are few studies in the literature about the effect of inter-layer transition time on quantum well, multilayer structures and lattice-match InGaAs/InAlAs QCL [17]. However, transition time studies have not been performed for strain-compensated QCL structures to the best of our knowledge.

In this study, we have been examined the optimization studies of the combination of Si-doped and undoped inter-layer transition time in the strain compensated $In_{0.67}Ga_{0.33}As/In_{0.36}Al_{0.64}As$

* Corresponding author.
E-mail address: idemir@cumhuriyet.edu.tr (I. Demir).

https://doi.org/10.1016/j.molstruc.2022.134203
0022-2860/

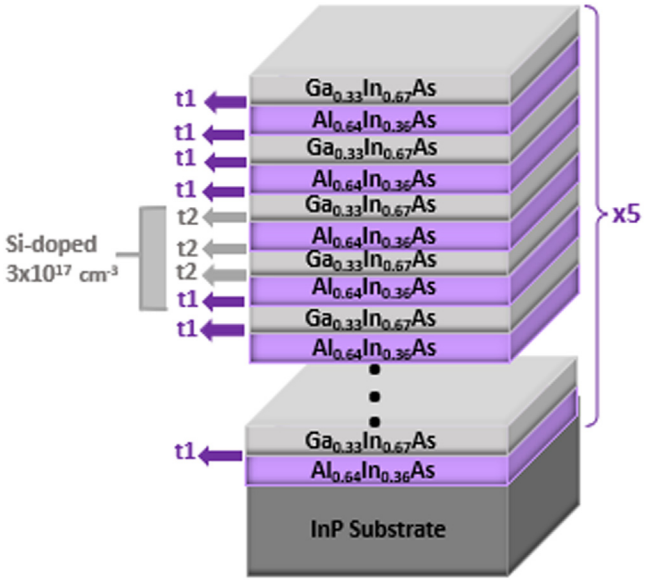

Fig. 1. Schematic representation strain-compensated of QCL structure grown on an InP substrate by MOVPE

QCL structure grown on InP substrate by MOVPE. After growth, the crystalline quality and thickness sensitivity of the samples have been investigated by HRXRD. In addition, two different calculation methods have been made from the Global Fit simulation program in order to examine the thickness sensitivities of the grown samples in more detail.

2. Experimental

InGaAs/InAlAs superlattice (SL) structures have been grown on InP (001) substrate by AIXTRON 200/4 RF-S MOVPE system. The metal-organic compounds TMIn (trimethylindium), TMAl (trimethylaluminum), and TMGa (trimethylgallium) have been used as In (indium), Al (aluminum), and Ga (gallium) precursors, respectively. High purity arsine (AsH_3) hydride, an inorganic compound, has been used as the source of As (arsenic). In addition, high purity silane (SiH_4) has been used for the Si-doped InGaAs and InAlAs layers. Growth parameters such as growth temperature, V/III ratio, and source flows have been optimized to achieve the desired crystalline quality and target alloy composition values. The flow rates of TMIn, TMAl, and AsH_3-2 have been used for growth of the InGaAs/InAlAs layer are 35 sccm, 12.5 sccm, and 15.1 sccm, respectively. The flow rates of TMIn, TMGa, and AsH_3-1 have been used for growth of the InGaAs layer are 35 sccm, 0.3 sccm, and 31 sccm, respectively. For InGaAs and InAlAs growths, the V/III ratios have been optimized as 128 and 45, respectively, and the growth temperature has been kept stable at 620°C for both layers. After many trials and optimization growths, $In_xGa_{1-x}As$ with x=0.67 In concentration and $In_yAl_{1-y}As$ single layers with y=0.36 In concentration on InP substrate successfully have been grown separately. Besides, for

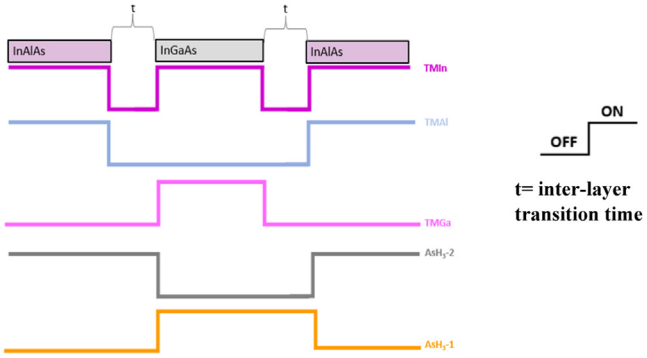

Fig. 3. Schematic representation of the source flow sequences of the gases used during growth and transition between layers

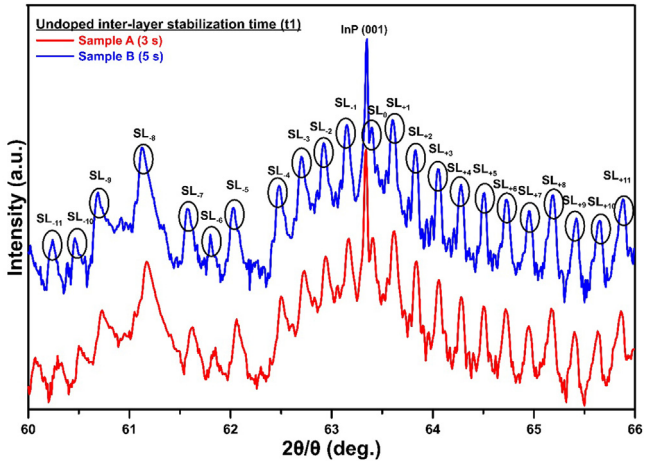

Fig. 4. HRXRD θ-2θ scans of Sample A and Sample B

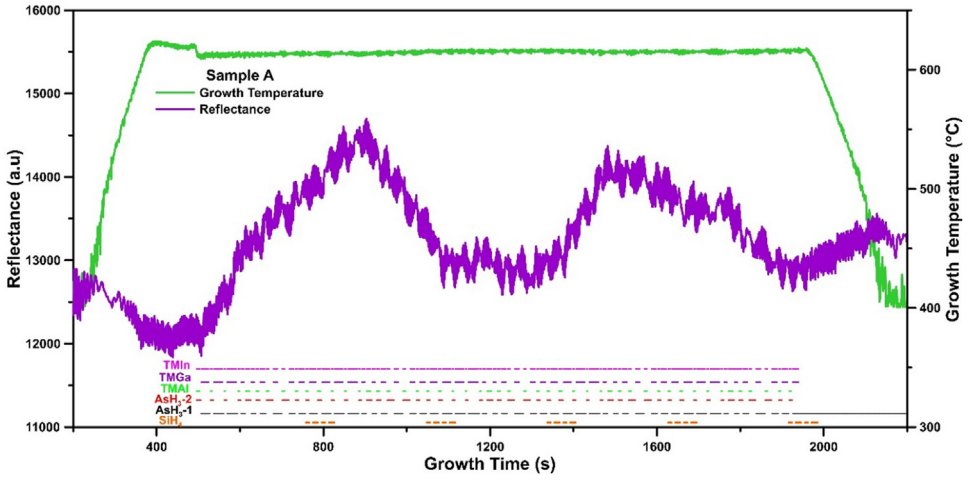

Fig. 2. The in situ reflectance and growth temperature versus growth time for Sample A.

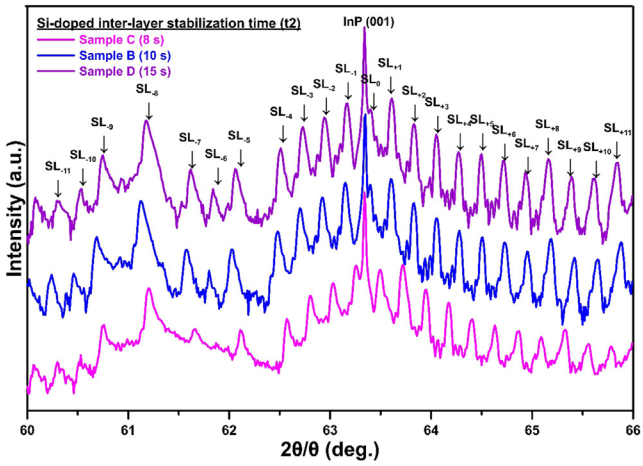

Fig. 5. HRXRD θ-2θ scans of Sample B, Sample C, and Sample D

the Si-doped InGaAs and InAlAs layers, SiH_4 flow rates have been changed and carrier densities of 3×10^{17} cm^{-3} have been obtained with a few optimization studies. The SiH_4 flow rates used for the Si-doped InGaAs and Si-doped InAlAs layers are 0.3 sccm and 1.4 sccm, respectively.

The core region of QCL structure is composed of 5 stages of the following sequence of lattice-mismatched $In_{0.67}Ga_{0.33}As/In_{0.36}Al_{0.64}As$ layers: **2.2**/3.7/**1.4**.....**1.7**/3 nm where

Table 1
Variation of t1 and t2 times of samples

Group 1 (t2 = 10 s)		Group 2 (t1 = 5s)		
Sample A	Sample B	Sample C	Sample B	Sample D
t1 = 3 s	**t1** = 5 s	**t2** = 8 s	**t2**= 10 s	**t2** =15 s

InAlAs layers are given in bold. Fig. 1 shows a schematic representation of the strain compensated QCL structure grown by MOVPE on an InP substrate. The inter-layers stabilization times have been examined in 2 groups. The transition times between undoped and Si-doped layers are labeled as t1 and t2, respectively. In the first group, t2 (10 s) time has been kept constant, while t1 time has been changed to 3 and 5 s for Sample A and B, respectively. In the second group, t1 (5 s) time has been kept constant and t2 time has been changed to 8, 10 and 15 s for Samples C, B and D. The variation of t1 and t2 times for all samples is given in Table 1.

3. Results and discussion

In-situ characterization is a very effective and practical measurement technique that provides information about growth rate, layer thickness and surface condition during epitaxial growth [19,20]. In order to observe the growth transitions and their effects during the growth of InGaAs and InAlAs layers, a semiconductor laser operating at 880 nm wavelength has been used as an in situ monitoring system. Fig. 2 shows the in-situ reflectance and growth temperature versus growth time for Sample A. Since the in-situ re-

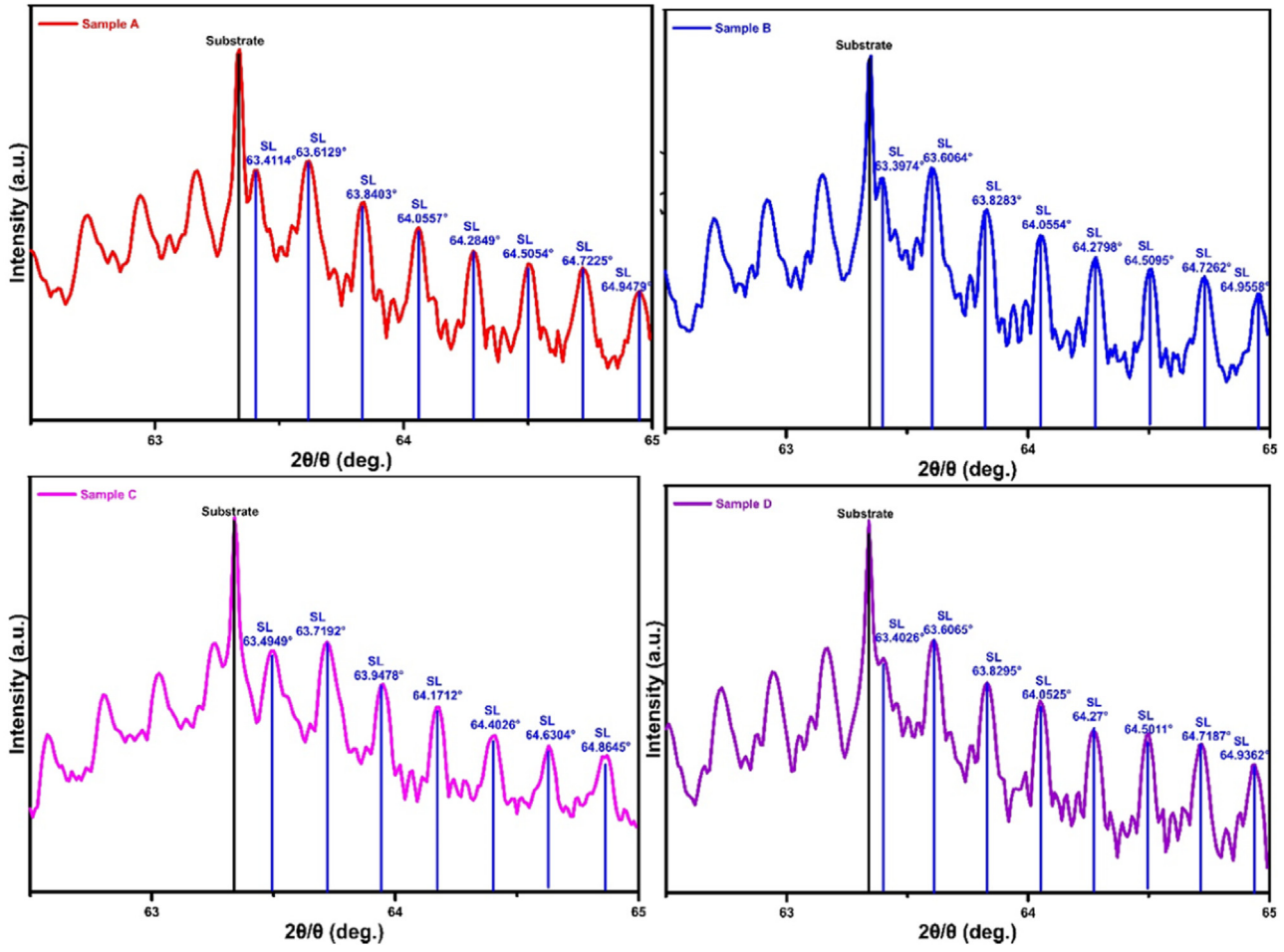

Fig. 6. Period thickness calculation of Sample A, Sample B, Sample C, and Sample D with Global Fit simulation program

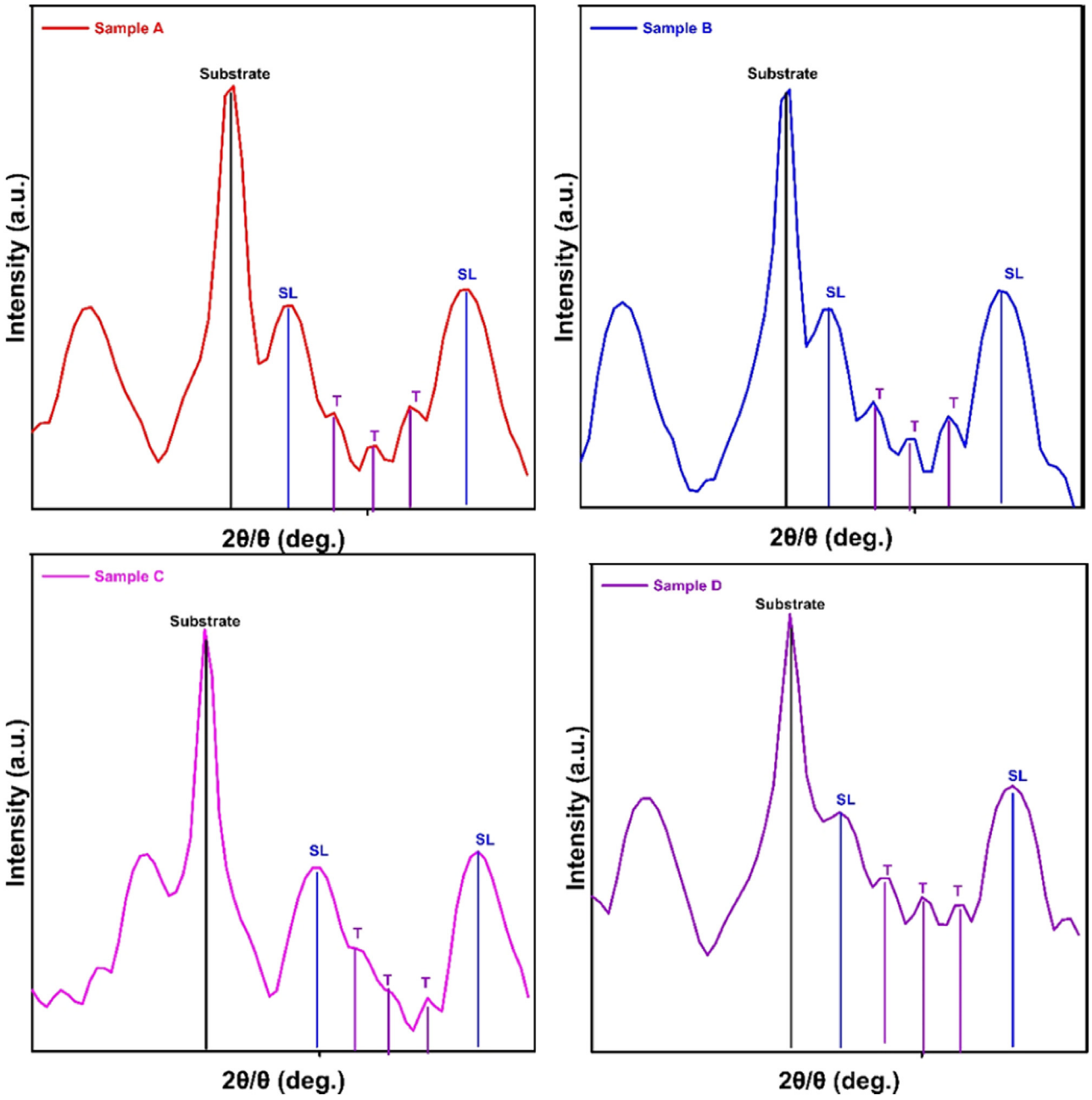

Fig. 7. Total layer thickness calculation of Sample A, Sample B, Sample C, and Sample D with Global Fit simulation program

flectance behavior has been almost the same in all samples, only the measurement of Sample A have been examined. Due to the refractive index difference of the $In_{0.67}Ga_{0.33}As$ and $In_{0.36}Al_{0.64}As$ layers, the in-situ reflectance behavior is different and each step of growth can be distinguished in the reflectance measurement. As the thicknesses of the $In_{0.67}Ga_{0.33}As$ and $In_{0.36}Al_{0.64}As$ layers in each repeat has been different, an asymmetric behavior has been observed in the reflectance curve. The flow times and states of sources used during growth and inter-layer transition are also inside of figure.

In Fig. 3, the source flow sequence of the InAlAs and then the InGaAs layers have been given in detail for a better understanding of the growth. Two separate AsH_3 lines have been used to make a rapid transition between the optimized V/III ratios obtained for the InGaAs and InAlAs layers. The gases released at $In_{0.36}Al_{0.64}As$ growth are TMIn, TMAl and AsH_3-2. While TMIn and TMAl are closed when the growth is finished, AsH_3-2 gas is left open until $In_{0.67}Ga_{0.33}As$ growth starts in order to prevent the escape of As atoms from the grown surface. When $In_{0.67}Ga_{0.33}As$ growth starts, AsH_3-2 flow is stopped and TMIn, TMGa and AsH_3-1 flows are provided. AsH_3-1 flow continues until $In_{0.36}Al_{0.64}As$ growth is initiated again. This process continues until the growth has been completed in the same way.

The HRXRD technique provides information on the structural properties of epitaxial layers [21,22]. The $2\theta/\theta$ HRXRD scan has been performed in the range of 2θ = 60-66° to investigate the effect of the variation of t1 and t2 time on the crystalline quality and thickness sensitivity of the structures, is shown in Figs. 4 and 5. As shown in Fig. 4, the positions of the SL peaks are almost in match with each other for both samples. If smaller angles ($2\theta <$ 63.3°) have been examined the superlattice (SL) peaks of the measured curve for Sample A become slightly broadened and the in-

tensity decreases compared to Sample B. More intensity and periodic SL peaks indicate better crystalline quality, so Sample B has better crystalline quality. As shown in Fig. 5, although the SL positions of Sample B and Sample D match each other, Sample C is not in agreement. Compared to the other two samples, the SL peaks of Sample C have less intensity. In addition, the thickness fringes are not clearly evident like other samples. This means that there is lattice defect including mismatch locations, rough interfaces, and compositional fluctuation. Although the SL peak intensity and positions are almost the same in samples B and D, it is necessary to compare the thickness sensitivities of the samples. It is impractical to extend the growth time for the QCL active region containing hundreds of layers with very thin thicknesses. It is more ideal when we compare Sample B with D in terms of growth time.

In order to investigate the thickness sensitivities of the grown samples in more detail, two different calculation methods have been made from the Global Fit simulation program. First of all, periodicity analysis for satellite peaks method has been used to obtain the period thickness. In this method, the superlattice periodicity is calculated by considering the positions of the satellite peaks. A superlattice shows different diffraction pattern with satellite peaks are observed around the Bragg reflection of the primitive lattice. The following formula shows the relationship between the superlattice periodicity Λ and the angular position of a satellite peak.

$$\Lambda = \frac{(m-n)\lambda}{2\left(\sin\frac{2\theta_m}{2} - \sin\frac{2\theta_n}{2}\right)} \quad (1)$$

where λ is the wavelength of the x-ray, m and n the orders of satellite peaks, while $2\theta_m$ and $2\theta_n$ are angles of the corresponding peaks.

Fig. 6 shows the SL peak positions and corresponding angles of Samples A, B, C, and D. As a result of this simulation, period thickness values of all samples have been obtained. The period thickness values obtained for Samples A, B, C and D samples have been determined as 47.29, 46.13, 45.37 and 46.93 nm, respectively. The thickness of the target period for the QCL structure is 46.1 nm. As a result, the best thickness sensitivity has been successfully achieved for Sample B with a very small thickness difference of 0.03 nm.

The second method, analysis of thickness of epitaxial thin film method has been used to obtain the total layer thickness. The thickness of the epitaxial thin film can be calculated bottomed on the fringes from x-ray interference visible in the measurement profile. The epitaxial layer thickness D can be expressed using the fringe period $\Delta\omega$ as shown in the formula below.

$$D = \frac{\lambda\ |\gamma_h|}{\Delta\omega\ \sin 2\theta} \quad (2)$$

where θ is the Bragg angle, and λ is the wavelength of the x-ray. γ_h is the direction cosine of the plane normal and the vector of the diffracted x-ray.

Fig. 7 shows the positions of the two SL peaks and fringes between these peaks for Samples A, B, C, and D. In the figure, the fringes are indicated with "T". The total layer thickness values obtained for Sample A, B, C and D samples have been determined as 231.34, 229.71, 228.66 and 248.37 nm, respectively. The total thickness for the QCL structure is 230.5 nm. Consequently, with a thickness difference of 0.79 nm with the total layer thickness method, Sample B is the sample most match with the target thickness.

4. Conclusions

In this study, strain compensated $In_{0.67}Ga_{0.33}As/In_{0.36}Al_{0.64}As$ QCL structures have been grown with MOVPE on InP substrate and the interlayer transition times of grown samples have been examined in two groups as Si-doped layers and undoped layers. In-situ reflectance measurement has been used to examine the flow sequences of the sources and growth steps of structures. The HRXRD system has been used to examine the crystalline quality of the grown samples and the Global Fit simulation program has been used to analyze the thickness sensitivities in detail. With a small deviation of 0.03 nm in the period thickness results and a difference of 0.79 nm in the total layer thickness results, optimum values with the most accurate thickness sensitivity of un-doped and Si-doped inter-layer times of 5 s and 10 s have been obtained.

Declaration of Competing interest

The authors declare that they have no known competing financial interests or personal relationships that could have appeared to influence the work reported in this paper.

CRediT authorship contribution statement

Izel Perkitel: Writing – original draft, Investigation, Conceptualization. **Ilkay Demir:** Writing – review & editing, Supervision, Project administration, Methodology, Funding acquisition.

Data Availability

Data will be made available on request.

Acknowledgments

The authors acknowledge the usage of the Nanophotonics Research and Application Center at Sivas Cumhuriyet University (CUNAM) facilities. This work is supported by the Scientific Research Project Fund of Sivas Cumhuriyet University under the project number MRK-2022-003 and M-2022-841.

References

[1] A. Lyakh, R. Maulini, A. Tsekoun, R. Go, C. Pflügl, L. Diehl, C.K.N. Patel, 3 W continuous-wave room temperature single-facet emission from quantum cascade lasers based on nonresonant extraction design approach, Appl. Phys. Lett. 95 (14) (2009) 141113.
[2] J. Faist, F. Capasso, D.L. Sivco, C. Sirtori, A.L. Hutchinson, A.Y. Cho, Quantum cascade laser, Science 264 (5158) (1994) 553–556.
[3] P. Figueiredo, M. Suttinger, R. Go, E. Tsvid, C.K.N. Patel, A. Lyakh, Progress in high-power continuous-wave quantum cascade lasers, Appl. Opt. 56 (31) (2017) H15–H23.
[4] D.H. Kim, H.Y. Jeong, Y.S. Choi, D. Park, Y.J. Jeon, D.H. Jun, InGaAs/InAlAs quantum cascade lasers grown by using metal-organic vapor-phase epitaxy, Appl. Sci. Converg. Technol. 26 (5) (2017) 139–142.
[5] A. Kosterev, G. Wysocki, Y. Bakhirkin, S. So, R. Lewicki, M. Fraser, R.F. Curl, Application of quantum cascade lasers to trace gas analysis, Appl. Phys. B 90 (2) (2008) 165–176.
[6] F.K. Tittel, D. Richter, A. Fried, Solid state mid-infrared laser sources, in: I.T. Sorokina, K.L. Vodopyanov (Eds.), Topics Appl. Phys., Springer, Berlin New York, 2003, pp. 445–510. vol. 89.
[7] R.F. Curl, F.K. Tittel, 7 Tunable infrared laser spectroscopy, Ann. Rep. Section" C"(Phys. Chem.) 98 (2002) 219–272.
[8] S. Blaser, D. Hofstetter, M. Beck, J. Faist, Free-space optical data link using Peltier-cooled quantum cascade laser, Electron. Lett. 37 (12) (2001) 778–780.
[9] D. Hofstetter, M. Beck, J. Faist, M. Nägele, M.W. Sigrist, Photoacoustic spectroscopy with quantum cascade distributed-feedback lasers, Opt. Lett. 26 (12) (2001) 887–889.
[10] N. Mustafa, L. Pesquera, C.Y.L. Cheung, K.A. Shore, Terahertz bandwidth prediction for amplitude modulation response of unipolar intersubband semiconductor lasers, IEEE Photon. Technol. Lett. 11 (5) (1999) 527–529.
[11] M.P. Semtsiv, M. Ziegler, S. Dressler, W.T. Masselink, N. Georgiev, T. Dekorsy, M. Helm, Above room temperature operation of short wavelength ($\lambda = 3.8\ \mu$m) strain-compensated In 0.73 Ga 0.27 As–AlAs quantum-cascade lasers, Appl. Phys. Lett. 85 (9) (2004) 1478–1480.
[12] S. Blaser, D.A. Yarekha, L. Hvozdara, Y. Bonetti, A. Muller, M. Giovannini, J. Faist, Room-temperature, continuous-wave, single-mode quantum-cascade lasers at $\lambda \simeq 5.4\ \mu$ m, Appl. Phys. Lett. 86 (4) (2005) 041109.
[13] M. Beck, D. Hofstetter, T. Aellen, J. Faist, U. Oesterle, M. Ilegems, H. Melchior, Continuous wave operation of a mid-infrared semiconductor laser at room temperature, Science 295 (5553) (2002) 301–305.
[14] R. Maulini, A. Lyakh, A. Tsekoun, C.K.N. Patel, $\lambda \sim 7.1\ \mu$m quantum cascade lasers with 19% wall-plug efficiency at room temperature, Opt. Express 19 (18) (2011) 17203–17211.

[15] W.T. Masselink, M.P. Semtsiv, S. Dressler, M. Ziegler, N. Georgiev, T. Dekorsy, M. Helm, High-power short-wavelength quantum cascade lasers. In *Novel In–Plane Semiconductor Lasers IV*, Int. Soc. Optics Photonics 5738 (2005) 13–24.
[16] J. Faist, F. Capasso, D.L. Sivco, A.L. Hutchinson, S.N.G. Chu, A.Y. Cho, Short wavelength ($\lambda\sim$ 3.4 μm) quantum cascade laser based on strained compensated InGaAs/AlInAs, Appl. Phys. Lett. 72 (6) (1998) 680–682.
[17] I. Demir, S. Elagoz, Interruption time effects on InGaAs/InAlAs superlattices of quantum cascade laser structures grown by MOCVD, Superlattices Microstruct. 100 (2016) 723–729.
[18] A. Łozińska, M. Badura, K. Bielak, B. Ściana, M. Tłaczała, The influence of quantum well and barrier thicknesses on photoluminescence spectra of InGaAs/AlInAs superlattices grown by LP-MOVPE, Optica Applic. 50 (2) (2020).
[19] İ. PERKİTEL, İ. ALTUNTAS, İ DEMİR, The effect of Si (111) substrate surface cleaning on growth rate and crystal quality of MOVPE grown AlN, in: Gazi Univ. J., 35, 2022, pp. 281–291.
[20] G. Yolcu, I. Simsek, R. Kekul, I. Altuntas, S. Horoz, I. Demir, The influence of TMGa pre-flow time and amount as surfactant on the structural and optical properties of AlN epilayer, Micro Nanostruct., 2022.
[21] M.N. Koçak, K.M. Pürlü, İ. Perkitel, İ. Altuntaş, İ. Demir, *In-situ* and ex-situ face–to-face annealing of epitaxial AlN, Vacuum 203 (2022) 111284.
[22] K.M. Pürlü, M.N. Koçak, G. Yolcu, İ. Perkitel, İ. Altuntaş, I. Demir, Growth and characterization of PALE Si-doped AlN on sapphire substrate by MOVPE, Mater. Sci. Semicond. Process. 142 (2022) 106464.

Filters Clear All

- *Web of Science* Coverage
- Open Access
- Category
- Country / Region
- Language
- Frequency
- Journal Citation Reports

Refine Your Search Results

Journal of Molecular Structure Search

Sort By: Relevancy

Search Results

Found 960 results (Page 1) Share These Results

Exact Match Found

JOURNAL OF MOLECULAR STRUCTURE

Publisher: **ELSEVIER , RADARWEG 29, AMSTERDAM, Netherlands, 1043 NX**

ISSN / eISSN: **0022-2860 / 1872-8014**

Web of Science Core Collection: **Science Citation Index Expanded**

Additional *Web of Science* Indexes: **Current Contents Physical, Chemical & Earth Sciences | Essential Science Indicators**

Share This Journal View profile page

** Requires free login.*

Other Possible Matches

NATURE STRUCTURAL & MOLECULAR BIOLOGY

Publisher: **NATURE PORTFOLIO , HEIDELBERGER PLATZ 3, BERLIN, Germany, 14197**

ISSN / eISSN: **1545-9993 / 1545-9985**

Web of Science Core Collection: **Science Citation Index Expanded**

Additional *Web of Science* Indexes: **Biological Abstracts | BIOSIS Previews | Current Contents Life Sciences | Essential Science Indicators**

Share This Journal View profile page

** Requires free login.*

ALGORITHMS FOR MOLECULAR BIOLOGY

OPEN ACCESS

Publisher: **BMC , CAMPUS, 4 CRINAN ST, LONDON, ENGLAND, N1 9XW**